Indian J. Phys. **79** (11), 1237-1241 (2005)

A modified gravitational potential to study particles and fluids around a rotating black hole in the equatorial plane

Sandip K Chakrabarti[1,2*] and Soumen Mondal[1]

[1] S. N. Bose National Centre for Basic Sciences,
JD-Block, Sector-III, Salt Lake, Kolkata-700 098, India
[2]Centre for Space Physics, 43 Chalantika, Garia Station Road, Kolkata-700 084, India

E-mail: chakraba@bose.res.in

Received 7 September 2005, accepted 23 September 2005

Abstract : Studies of the particle trajectories and the fluid dynamics around a Schwarzschild black hole are regularly carried out usinga so-called Paczynski-Wiita potential. In the present communication, we give a form of the potential, valid on the equatorial plane, which is suitable for the study of the particles around a rotating black hole. We show that the salient features of the orbits, such as the marginally bound orbit and the marginally stable orbit match with those obtained from exact consideration very accurately, provided $-1 \geq a \geq 0.8$. A comparison of the nature of the potentials also reveals that they are similar. We believe that this pseudo-Newtonian approach would be very valuable in the future study of various phenomena such as the spectra, time dependent solutions through numerical simulations, Quasi-Periodic Oscillations of observed X-rays *etc* in accretion disks around rotating black holes.

Keywords : Black holes, particles trajectories

PACS Nos. : 04-20-q, 04.70.Bw, 83.10.Pp, 02.60.Cb

1. Introduction

It is customary in the astrophysical literature to use a pseudo-Newtonian description of the space-time in which the gravitational potential $\Phi_N(r) = -GM/r$ is replaced by the pseudo-Newtonian (PN) potential $\Phi(r)_{PN} = -GM/(r-2GM/c^2)$, originally proposed by Paczyński and Wiita [1]. Here, G and c are the universal gravitational constant and the velocity of light, respectively and M is the mass of the black hole. The idea of choosing this potential is that in this case, if one calculates the specific angular momentum $l(r)$ needed to stay in a circular orbit of radius r by equating the centrifugal acceleration with the gravitational acceleration :

$$\frac{l(r)^2}{r^3} = \frac{GM}{r\left(r-2GM/c^2\right)^2}, \qquad (1)$$

then, one obtains the so-called Keplerian distribution

$$l_{Kep}(r) = \frac{\left[GMr^3\right]^{1/2}}{\left[r-\frac{2GM}{c^2}\right]} \qquad (2)$$

which is *identical* to the distribution of the circular time-like geodesics around a Schwarzschild black hole. This so-called pseudo-Newtonian potential allows one to use Newtonian equations to describe the particle and fluid behaviour around a non-rotating black hole. While it is relatively easy to study particle trajectories (*e.g.*, Chandrasekhar [2]), and fluid dynamics for adiabatic flows in full general relativity (*e.g.*, Chakrabarti [3]), it is prohibitive to do theoretical studies and numerical simulations, particularly in presence of heating, cooling and magnetic fields, using full general relativistic formalism. From the observational point of view, since most of the photons which are detected through telescopes, arise out of the disk regions away from the marginally stable orbits ($r > r_{ms}$), it is usually sufficient to restrict the studies of the disks for $r > r_{ms}$. For instance, the inner edge of a standard Keplerian disk is located at $r = r_{ms}$. The errors made using pseudo-Newtonian

* Corresponding Author

approach is also a few percent which is not distinguishable through present day observations. Thus, unless one makes a very strong statement about detecting the horizon, our approach should be very useful.

In this *Rapid Communication*, we plan to present a 'pseudo-Newtonian'potential so as to carry out the particle dynamical study around a Kerr geometry. The philosophy of writing such a potential is to carry out Newtonian calculations using such a potential that as seen from a distant observer, the general relativistic trajectories match with the 'pseudo-Newtonian' trajectories. For the present, we write down the equations only on the equatorial plane so that equatorial orbits and thin accretion flows may be studied. In future, we shall generalize the potential away from the equatorial plane so that we may be able to study thick accretion flows as well.

In the next Section, we present the properties of equatorial orbits in Kerr geometry. In Section 3, we present our potential and in Section 4, we discuss the locations of the marginally bound and marginally stable orbits as obtained from our potential. We also present the comparison between these orbital locations. We compare the nature of the effective potentials (*i.e.* gravitational plus centrifugal) and show that they are also almost identical. Finally, in Section 5, we draw our conclusions.

2. Marginally bound and marginally stable orbits in Kerr geometry

In what follows, we choose $G = c = M = 1$. The distances, specific angular momenta and times are measured in units of GM/c^2, GM/c and GM/c^2, respectively. Before we discuss what the effective potential should be, we need to remind ourselves some of the properties of the Kerr geometry on the equatorial place. The stationary and axisymmetric metric in the Boyer-Lindquist coordinate (t, r, θ, ϕ) with $\theta = \pi/2$ is given by (see, *e.g.*, Shapiro and Teukolsky, [4])

$$ds^2 = -\left(1 - \frac{2}{\Sigma}\right)dt^2 - \frac{4ar}{\Sigma}dtd\phi + \frac{\Sigma}{\Delta}dr^2 + \left(r^2 + a^2 + \frac{2ra^2}{\Sigma}\right)d\phi^2, \quad (3)$$

where $a = J / M$ is the Kerr parameter, $\Delta = r^2 - 2r + a^2$ and $\Sigma = r^2 + a^2$.

From the Lagrangian L on the equatorial plane,

$$2L = -\left(1 - \frac{2}{r}\right)\dot{t}^2 - \frac{4a}{r}\dot{t}\dot{\phi} + \frac{r^2}{\Delta}\dot{r}^2 + \left(r^2 + a^2 + \frac{2a^2}{r}\right)\dot{\phi}^2, \quad (4)$$

where dots represent derivatives with respect to an affine parameter along the curve, one can obtain the equations of motion of test particles. From this, one obtains the two conserved quantities corresponding to two ignorable co-ordinates, namely,

$$p_t = \frac{\partial L}{\partial \dot{t}} = -E, \quad (5a)$$

and

$$p_\phi = \frac{\partial L}{\partial \dot{\phi}} = l'. \quad (5b)$$

The third integral is obtained from $g_{\alpha\beta}p^\alpha p^\beta = -m^2$, *i.e.*, $L = -m^2/2$ [4]. This gives rise to the radial equation of motion

$$r^3\dot{r}^2 = R(E, l, r),$$

where

$$R = E^2\left(r^3 + a^2r + 2a^2\right) - 2aEl' - (r-2)l'^2 - m^2r\Delta. \quad (6)$$

The existence of the metric element gives rise to the so-called spin-orbit coupling term containing the product *al* which is crucial to distinguish between co-and contra-rotating orbits. A second important feature that arises is the existence of a 'red-shift' factor with the rotational kinetic energy term. For circular orbits, $\dot{r} = 0$, which implies *R* equals to zero and one can obtain the locations of the marginally bound and marginally stable orbits in the following way: The locations of the marginally bound and marginally stable circular orbits occur at extremal values of the function *R*. Thus,

$$\frac{\partial R}{\partial r} = 0.$$

This condition together with $R = 0$ gives

$$\tilde{E} = r^2 - 2r \pm a\sqrt{r}\Big/\left(r^{3/2} - 3r \pm 2a\sqrt{r}\right)^{1/2},$$

$$\tilde{l} = \pm\sqrt{r}\left(r^2 \mp 2a\sqrt{r} + a^2\right)\Big/\left(r^{3/2} - 3r \pm 2a\sqrt{r}\right)^{1/2},$$

where $\tilde{E} = E/m$ and $\tilde{l} = l/m$.

Here, + ve sign is for co-rotating and – ve sign is for the counter-rotating orbits. By putting $\tilde{E} = E/m = 1$, the solution for marginally bound circular orbit is

$$r_{mb} = 2 \mp a + 2\sqrt{(1 \mp a)}.$$

For $a = 0$, $r_{mb} = 4$; for $a = 1$, $r_{mb} = 1$ (direct) or 5.83 (retrograde).

The radius of the marginally stable circular orbits occurs at the point of inflexion, which requires

$$\partial^2 R/\partial r^2 = 0.$$

Thus, the expression for marginally stable circular orbit r_{ms} , is given by,

$$r_{ms} = 3 + D_2 \mp \sqrt{[(3 - D_1)(3 + D_1 + 2D_2)]},$$

where

$$D_1 = 1 + \left(1 - a^2\right)^{1/3}\left[(1+a)^{1/3} + (1-a)^{1/3}\right],$$

$$D_2 = \sqrt{(3a^2 + D_1^2)}\,.$$

For $a = 0$, $r_{ms} = 6$; for $a = 1$, $r_{ms} = 1$ (direct) or 9 (retrograde).

3. Pseudo-Kerr potential on the equatorial plane

In order to write an effective pseudo-Newtonian potential, it must be remembered that it should contain additive terms coming from various forms of energies, such as the gravitational energy, rotational energy and the energy due to coupling of the spin and orbital angular momentum. The potential we propose is :

$$\Phi(r) = 1 - \frac{1}{r - r_0} + \frac{2a\left(\tilde{l} + \omega r^2\right)}{r^2} + \alpha^2 \frac{\left(\tilde{l} + \omega r^2\right)}{2r^2}, \quad (7)$$

where $r_0 = 0.04 + 0.97a + 0.085a^2$, α , the redshift factor, in Kerr geometry is given by

$$\alpha = \frac{r}{\Sigma}\sqrt{\Delta}\,, \quad (8a)$$

where, $\Sigma^2 = \left(r^2 + a^2\right) - a^2\Delta,\ \Delta = r^2 + a^2 - 2r$, and $\tilde{l} = \dot{\phi}_0 r^2$.

The coordinate ϕ_0 can be attached to the zero-angular momentum observers. We shall use the convention that for retrograde orbits, negative *a* would be used and $\tilde{l}$ would always be chosen to be positive. Here, the red-shift factor α [eq. (8a)] and the dragging term, ω have been borrowed from general relativity

$$\omega = \frac{2ar}{\left(r^2 + a^2\right) - \Delta a^2}. \quad (8b)$$

The specific angular momentum $\tilde{l}$ here has the same meaning as u_ϕ in GTR.

The form of the potential [eq. (7)] is to be compared with what is used in the Newtonian geometry, the effective potential around a star of mass *M* is given by

$$\Phi_N = -\frac{1}{r} + \frac{1}{2}\,\frac{l^2}{r^2}\,, \quad (9a)$$

or that around a pseudo-Newtonian geometry [Paczynski and Wiita, (1980)]

$$\Phi_{PW} = -\frac{1}{r-2} + \frac{1}{2}\,\frac{l^2}{r^2}\,, \quad (9b)$$

which is widely used for studies around a Schwarzschild black hole. It is to be noted that *l* here should be compared with $l = -u_\phi / u_t$ in GTR. Because of this difference in definitions, the singularity at $r = 2$ in eq. (9b) is not evident in eq. (7) when the special case of $a = 0$ is considered.

It is easy to understand the meaning of the individual terms of our effective potential. The first term corresponds to the rest mass energy and the second term gives rise to a singularity at $r = r_0$. $r = r_0$ is not the horizon, but the constant r_0 was adjusted in a way that the major properties of the orbits, such as, the locations of marginally bound and marginally stable orbits, remain roughly unchanged. The third term is due to the spin-orbit coupling term. Because the frame is dragged even when the specific angular momentum is zero, the effect of this dragging term (ω) has been added up with the term containing the orbital angular momentum. The same argument has been used to formulate the rotational energy term [fourth term in eq. (7)]. We have chosen r_1 exactly in analogy with the spin-orbit coupling term in a hydrogen atom.

There are two geometric length scales in a Kerr geometry which are (a) the horizon $r_+ = 1 + (1 - a^2)^{1/2}$ in units of GM/c^2 and (b) the ergosphere = $2GM/c^2$. We do not have an explicit location like a horizon, but our potential becomes singular at $r = r_0$. We also have a radius similar to the ergosphere : If we define the azimuthal coordinate ϕ_0 attached to the particle which is measured by a distant observer, then ϕ_0 and ϕ_d are related through

$$\dot{\phi}_d = \alpha^2 \dot{\phi}_0 + \alpha^2 \omega + \frac{2a}{r}\,. \quad (10)$$

For the existence of an 'ergosphere', there must be some $r = r_e$, such that $\dot{\phi}_d \leq 0$ at r_e. It is easily proven that up to an order of $a / l^2 << 1$, $r_e \leq 2a / l < 2$. This shows that the potential also exhibits such a radius, though its location depends on *a* and *l*. In reality, we are not concerned about these deviations as for astrophysical observational purposes, we will be away from marginally stable orbits anyway.

4. Marginally bound and marginally stable orbits for Pseudo-Kerr Potential

One can compute the locations of the marginally stable (ms) orbit by usual procedure, namely, by taking the radial derivative

of the Psuedo-Kerr potential twice and then setting both the first and the second derivatives to zero. The radius at which the point of inflexion of the potential occurs is the marginally stable orbit. Mathematically,

$$\left.\frac{d\Phi}{dr}\right|_{r_{ms}} = 0 .$$

This means that at $r = r_{ms}$,

$$\frac{1}{(r-r_0)^2}+\frac{2ag(r)}{r^3}\left(-\frac{3}{r}+\frac{g'(r)}{g(r)}\right)+\frac{\alpha^2 g(r)^2}{r^2}\times\left(-\frac{1}{r}+\frac{\alpha'}{\alpha}+\frac{g'(r)}{g(r)}\right)=0 , \qquad (11a)$$

and $$\left.\frac{d^2\Phi}{dr^2}\right|_{r_{ms}} = 0,$$

i.e. at $r = r_{ms}$,

$$\frac{-2}{(r-r_0)^3}+\frac{2ag(r)}{r^3}\left(\frac{g'(r)}{g(r)}-\frac{3}{r}\right)+\left(\frac{g''(r)}{g(r)}-\frac{6}{r^2}-\frac{g'(r)^2}{g(r)^2}-\frac{9}{r^2}\right)+\frac{\alpha^2 g(r)^2}{r^2}\left(\frac{\alpha'}{\alpha}+\frac{g'(r)}{g(r)}-\frac{1}{r}\right)^2+\left(\frac{\alpha''}{\alpha}+\frac{g''(r)}{g(r)}-\frac{\alpha'^2}{\alpha^2}+\frac{g(r)^2}{g(r)}+\frac{1}{r^2}\right)=0 , \qquad (11b)$$

where

$$g(r) = (1+\omega r^2) \text{ and } g'(r) = \omega' r^2 + 2\omega r .$$

Here, prime denotes the derivative with respect to r.

The angular momentum of a closed circular orbit at $r = r_{ms}$, is known as the marginally stable angular momentum l_{ms}. For the marginally bound orbits, one must have

$$\left.\frac{d\Phi}{dr}\right|_{r_{mb}} = 0,$$

i.e. at $r = r_{mb}$,

$$\frac{1}{(r-r_0)^2}+\frac{2ag(r)}{r^3}\left(-\frac{3}{r}+\frac{g'(r)}{g(r)}\right)+\frac{\alpha^2 g(r)^2}{r^2}\left(-\frac{1}{r}+\frac{\alpha'}{\alpha}+\frac{g'(r)}{g(r)}\right)=0 , \qquad (12a)$$

and

$$\Phi|_{r_{mb}} = 1 ,$$

i.e. at $r = r_{mb}$,

$$-\frac{1}{r-r_0}+\frac{2a(1+\omega r^2)}{r^3}+\frac{\alpha^2(1+\omega r^2)}{2r^2}\Bigg|_{r_{mb}} = 0 . \qquad (12b)$$

The angular momentum of a close circular orbit at $r = r_{mb}$, is known as the marginally bound angular momentum l_{mb}.

Figures 1(a, b) show the comparison of (a) r_{ms} and r_{mb}, (b) l_{ms} and l_{mb}; the solid curves are drawn using the Kerr solution while the dashed curves are drawn using the pseudo-Kerr potential. Clearly, the results agree reasonably well for the range

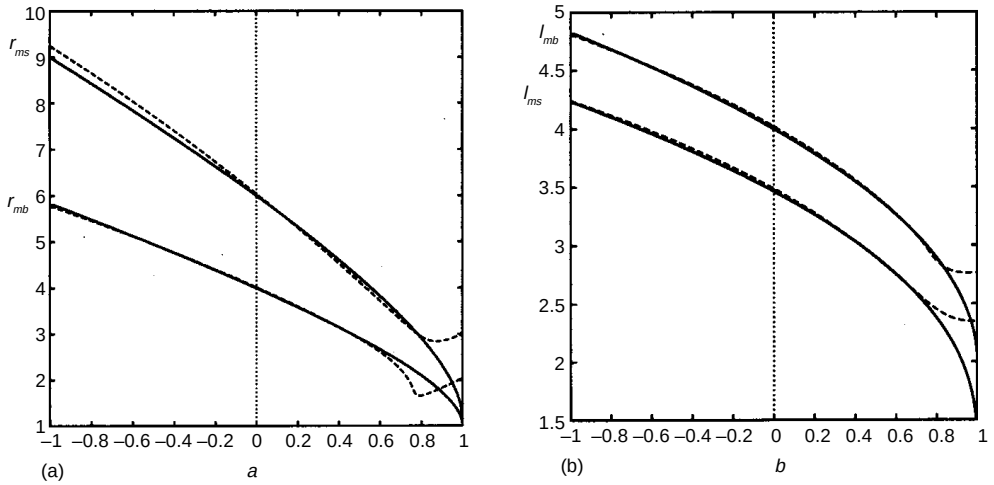

Figure 1. (a) The locations of the marginally bound (r_{mb}) and marginally stable (r_{ms}) orbits and (b) the angular momenta l_{mb} and l_{ms} at these orbits in both Kerr geometry (solid) and pseudo-Kerr geometry (dashed). Results generally agree for $-1 < a < 0.8$.

$-1 < a < 0.8$. The results at marginally bound orbit differs significantly for $a \sim 0.8$. However, for fluid dynamics of accretion disks (which will be dealt with elsewhere), the marginally stable orbits are more important than the marginally bound orbits. In any case, extremely rotating black holes *i.e.* those with $a \sim 1$, cannot be studied using our potential.

So far, the comparisons have been made for the parameters relevant for circular orbits. For elliptical orbits, the most important aspect that is relevant, is the nature of the effective potential. In Figure 2 (a, b), the potentials are drawn using (a) Kerr, and (b) pseudo-potential $\Phi(r)$ given by eq. (7). The lower and upper solid curves are drawn for the marginally stable and marginally bound angular momenta taken from Figure 1b. Other curves are for the same l in both the cases. As can be seen, there is very little difference in the potential. Since for a given $\Phi(r)$ and l, there could be two intersections r_1 and r_2 at virtually identical locations which correspond to apoastron and periastron, we thus believe that the elliptical orbits are trivially reproduced using our potentials.

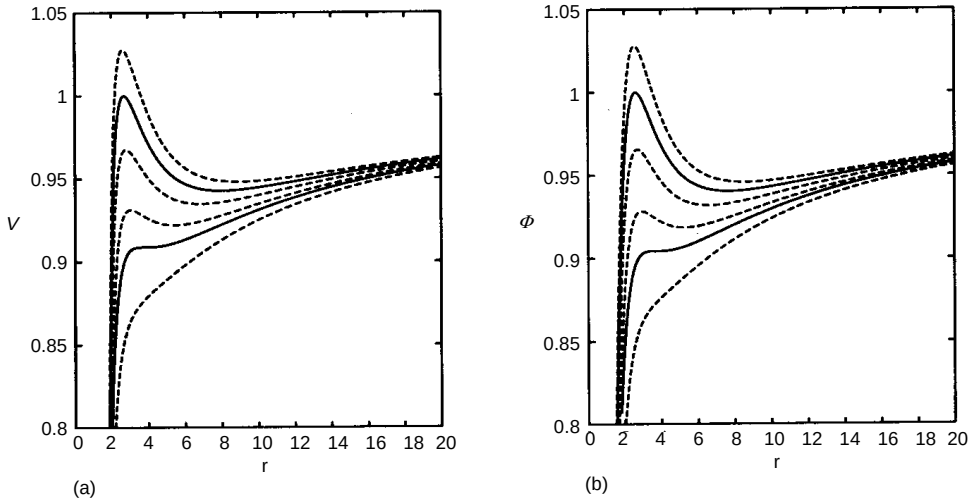

Figure 2. Comparison of (a) the General relativistic Kerr potential V_K and (b) the pseudo-Kerr potential Φ for a = 0.6. The lower solid curve is for marginally stable angular momentum and the upper solid curve is for the marginally bound angular momentum for the respective cases. Others curves are for the same angular momentum parameter l.

5. Summary

In this communication, we have presented a simple 'pseudo-Newtonian' potential to study particle trajectories around a rotating black hole. The reason why this potential deviates from $-1/r$ is that the nonlinear effects of the curvature of space-time are already incorporated into this potential. Thus, all the governing equations may be written in the same way as in the Newtonian space-time even though the orbital behaviour is that of a Kerr space-time. This methodology is well tested in Schwarzschild geometry in the past twenty five years or so where Paczyński-Wiita [1] potential was used. In the past [5], we also presented another form of the potential, and works have been done using that potential [6, 7] as well. However, the present form is much superior compared to the past efforts. Our effort here is to follow this technique for studying particle dynamics on the equatorial plane in a Kerr geometry for both the co-rotating and contra-rotating orbits. In future, we shall generalize this potential for non-equatorial orbits and also for fluids so that both theoretical and numerical studies may be made in the same spirit and with great ease.

References

[1] B Paczynski and P J Wiita *Astron. Astrophys.* **88** 23 (1980)

[2] S Chandrasekhar *Mathematical Theory of Black holes* (Oxford : Oxford Univ. Press) (1983)

[3] S K Chakrabarti *Mon. Not. Roy. Astron. Soc.* **283** 325 (1996)

[4] S L Shapiro and S A Teukolsky *Black Holes, White Dwarfs and Neutron Stars – the Physics of Compact Objects* (New York : John Wiley) (1983)

[5] S K Chakrabarti and R Khanna *Mon. Not. Roy. Astron. Soc.* **256** 300 (1992)

[6] R Khanna and S K Chakrabarti *Mon. Not. Roy. Astron. Soc.* **259** 1 (1992)

[7] D Molteni and H Sponholz *Mon. Not. Roy. Astron. Soc.* **271** 233 (1994)